Mon. Not. R. Astron. Soc. **000**, 000–000 (0000) Printed 21 August 2015 (MN LATEX style file v2.2)

Photon-conserving Comptonization in simulations of accretion disks around black holes

Aleksander Sądowski[1⋆] and Ramesh Narayan[1⋆]
[1] *MIT Kavli Institute for Astrophysics and Space Research, 77 Massachusetts Ave, Cambridge, MA 02139, USA*
[2] *Harvard-Smithsonian Center for Astrophysics, 60 Garden St., Cambridge, MA 02138, USA*

21 August 2015

ABSTRACT

We introduce a new method for treating Comptonization in computational fluid dynamics. By construction, this method conserves the number of photons. Whereas the traditional "blackbody Comptonization" approach assumes that the radiation is locally a perfect blackbody and therefore uses a single parameter, the radiation temperature, to describe the radiation, the new "photon-conserving Comptonization" approach treats the photon gas as a Bose-Einstein fluid and keeps track of both the radiation temperature and the photon number density. We have implemented photon-conserving Comptonization in the general relativistic radiation magnetohydrodynamical code KORAL and we describe its impact on simulations of mildly super-critical black hole accretion disks. We find that blackbody Comptonization underestimates the gas and radiation temperature by up to a factor of two compared to photon-conserving Comptonization. This discrepancy could be serious when computing spectra. The photon-conserving simulation indicates that the spectral color correction factor of the escaping radiation in the funnel region of the disk could be as large as 5.

Key words: accretion, accretion discs – black hole physics – relativistic processes – methods: numerical

1 INTRODUCTION

Accretion on black holes (BHs) is an important energy source that shapes the evolution of the Universe. Accreting supermassive BHs in the centers of galaxies expel a significant fraction of their accreted rest mass energy in the form of kinetic, thermal and radiative feedback, which affects the evolution of their host galaxies (e.g., Fabian 2012; King & Pounds 2015). At the same time, stellar mass BHs accreting in compact binaries, although not powerful enough to influence their hosts, are often the brightest X-ray sources in their galaxies.

For long our understanding of accretion was based on analytical models, most importantly the thin disk model of Shakura & Sunyaev (1973) and Novikov & Thorne (1973). Although such models provide important information on the dynamical properties of the accretion disk and predict its radiative luminosity, they provide only a rough idea of the emitted electromagnetic spectrum. To calculate the spectrum properly, including the effect of spectral hardening due to Comptonization in the strongly scattering medium, one has to solve the full radiative transfer problem for the disk atmosphere. Valuable work has been done in this area by Davis et al. (2005), who computed the vertical structure of disk atmospheres with a self-consistent treatment of radiative transfer. Their work made use of the code TLUSTY (Hubeny & Lanz 1995), with modifications to treat relativistic disks as described in Hubeny & Hubeny (1997) and Hubeny et al. (2001). Spectra obtained with this approach have been successfully used for modelling disk emission in the thermal-dominant (high/soft) state of X-ray binaries, and in particular for estimating BH spins via the continuum fitting method (e.g., McClintock et al. 2011).

The thin disk model can be applied only to optically thick, geometrically thin accretion flows. Once the accretion rate exceeds the Eddington rate, the various assumptions behind the thin disk model (e.g., radiative efficiency, Keplerian rotation) break down. Super-critical accretion flows have been modeled semi-analytically (Abramowicz et al. 1988; Sądowski 2011), but these models do not consistently account for mass outflows. In addition, although super-critical disks are known to be geometrically thick, their spectra have in the past been calculated using the plane-parallel approximation (see Straub et al. 2011), which is a gross simplifcation.

The proper, although computationally expensive, approach to modeling accretion disks is to simulate the accretion flow in multiple dimension, including angular momentum transport via magnetically-driven turbulence (Balbus & Hawley 1998), and to solve in parallel the multi-dimensional radiative transfer problem. Numerical codes to carry out such computations have become available only recently. Because of computational cost, often the radiative transfer in such simulations is simplified, and only in

⋆ E-mail: asadowsk@mit.edu (AS); rnarayan@cfa.harvard.edu (RN);

the postprocessing stage is the full, frequency dependent radiative tranport computed. The first magnetohydrodynamical numerical simulations of optically thick accretion disks, including radiation, were performed by Ohsuga et al. (2009) and Ohsuga & Mineshige (2011). These authors used a Newtonian approximation for gravity and modeled radiation under the flux limited diffusion approximation. In recent years, other groups have developed methods for general relativistic radiation-MHD simulations, including better radiation closures (Sądowski et al. 2013; McKinney et al. 2013; Fragile et al. 2014). Newtonian simulations with advanced radiative transport methods have also been carried out (Jiang et al. 2014a).

Super-critical accretion flows around stellar-mass BHs are very optically thick to electron scattering. They have temperatures of order a keV or more, so their absorption opacity is subdominant to scattering. As a result one expects significant Comptonization and spectral hardening of the escaping radiation. So far, however, simulations of super-critical disks have either ignored Comptonization altogether (Sądowski et al. 2014; Jiang et al. 2014b) or have treated it in a crude manner, which we call "blackbody Comptonization", in which the radiation is assumed to be locally a perfect blackbody (Kawashima et al. 2009; Sądowski et al. 2015a).

It might be hoped that it is sufficient to carry out simulations with the above "blackbody Comptonization," followed by a more detailed proper Comptonization calculation in a later postprocessing stage. However, as we show in this paper, the thermal state of the gas depends strongly on the particular implementation of Comptonization. The blackbody Comptonization approximation should therefore be treated with caution.

In this work we introduce an improved model of Comptonization in which we avoid the assumption that the local radiation at each point has a perfect blackbody spectrum. In the new method, we independently evolve both the radiation energy density and the photon number density, thereby relaxing the previous assumption that the two quantities are related precisely by the Planck function. To assess what effect this improvement in the modeling of Comptonization has, we have performed three simulations of a super-critical accretion disk, one with our previous "blackbody Comptonization," one with the improved "photon-conserving Comptonization" described in this paper, and one with no Comptonization at all. We compare the properties of the three simulations and draw conclusions.

The paper is organized as follows. In Section 2 we introduce the blackbody and photon-conserving versions of Comptonization. In Section 3 we give implementation details of the photon-conserving approach. In Section 4 we present the three simulations and analyze the results, and in Section 5 we briefly discuss the implications of the results.

2 COMPTONIZATION

2.1 Basic equations of GRRMHD

Within the framework of general relativity, the interaction between gas and radiation is described through the following general relativistic radiation magnetohydrodynamics (GRRMHD) conservation equations for gas density, ρ, and the stress-energy tensors, T^{μ}_{ν} and R^{μ}_{ν}, of the magnetized gas and radiation (Sądowski et al. 2013, 2014),

$$(\rho u^{\mu})_{;\mu} = 0, \tag{1}$$

$$(T^{\mu}_{\nu})_{;\mu} = G_{\nu}, \tag{2}$$

$$(R^{\mu}_{\nu})_{;\mu} = -G_{\nu}. \tag{3}$$

Here G^{ν} is the radiation four-force density acting on the gas. In orthonormal coordinates in the fluid (or gas) frame (denoted by hats), and in the absence of Comptonization, we have

$$\widehat{G^0} = \kappa_{\rm a}\rho(\widehat{E} - 4\pi\widehat{B}), \tag{4}$$

$$\widehat{G^i} = (\kappa_{\rm a} + \kappa_{\rm es})\rho\widehat{F^i}. \tag{5}$$

Here $\kappa_{\rm a}$ is the Rosseland mean absorption opacity (cross-sections per unit mass), which we adopt for simplicity instead of the proper absorption and Planck mean opacities. $\kappa_{\rm es}$ is the scattering opacity, $\widehat{E}$ is the radiative energy density in the fluid frame, $\widehat{B}$ is the intensity of blackbody radiation for gas of temperature $T_{\rm g}$,

$$\widehat{B} = \frac{aT_{\rm g}^4}{4\pi}, \tag{6}$$

where a is the radiation constant, and $\widehat{F^i}$ is the radiative flux three-vector.

Equation (4) describes the rate of change of the fluid energy density as a result of energy gain through absorption, $\kappa_{\rm a}\rho\widehat{E}$, and energy loss through emission, $\kappa_{\rm a}\rho(4\pi\widehat{B})$. The simplest approximation for modeling radiation is to treat it as a local blackbody at each point, so that the energy distribution is fully described by the local radiation temperature $T_{\rm r}$. In this approximation, the radiation energy density is given by

$$\widehat{E} = aT_{\rm r}^4. \tag{7}$$

Correspondingly, we rewrite equation (4) as

$$\widehat{G^0} = \kappa_{\rm a}\rho a(T_{\rm r}^4 - T_{\rm g}^4). \tag{8}$$

Equation (8) shows that gas gains energy at a rate proportional to $T_{\rm r}^4$ and loses energy proportional to $T_{\rm g}^4$. As a result, the two temperatures are pushed towards each other, i.e., the system is driven towards thermal equilibrium. Note that $\kappa_{\rm es}$ does not appear in the energy equation. For the present discussion, which ignores Comptonization, we have pure Thomson scattering, which only redirects photons but does not change photon energies.

Equation (5) describes the rate of change of the fluid momentum density. The gas acquires the momentum of each photon that it either absorbs or scatters. This explains the presence of both $\kappa_{\rm a}$ and $\kappa_{\rm es}$ in this equation. However, radiation that is emitted or scattered by the gas is symmetric in the fluid frame. Therefore, there is no corresponding momentum loss, hence no counter-balancing term with a negative sign. Note that the fluid gains momentum density in a direction parallel to the radiation flux three-vector $\hat{F}^i$, and the radiation loses a corresponding amount of momentum density. Hence the system is driven towards a state in which there is no relative motion between the fluid and radiation frames, i.e., no radiation flux in the fluid frame.

2.2 Thermal Comptonization: Blackbody Approximation

The main effect of Comptonization is that scattering causes not just momentum transfer between the radiation and gas, but also energy transfer. A soft photon of energy ϵ_0 which scatters off a thermal electron with temperature $T_{\rm e}$ on average gains an energy $\langle\Delta\epsilon\rangle$ given by the following expressions in the non-relativistic and ultra-relativistic limits, respectively (Rybicki & Lightman 1979),

$$\langle\Delta\epsilon\rangle = \left(\frac{4kT_{\rm e}}{m_{\rm e}c^2}\right)\epsilon_0, \qquad 4kT_{\rm e} \ll m_{\rm e}c^2, \tag{9}$$

$$\langle\Delta\epsilon\rangle = \left(\frac{4kT_{\rm e}}{m_{\rm e}c^2}\right)^2\epsilon_0, \qquad 4kT_{\rm e} \gg m_{\rm e}c^2. \tag{10}$$

For a general temperature, the result is given in equation (2.43) in Pozdnyakov et al. (1983). A good fitting function (maximum fractional error 1.2%) is the following:

$$\langle \Delta\epsilon \rangle = \epsilon_0 \left(\frac{4kT_{\rm e}}{m_{\rm e}c^2}\right)\left[1 + 3.683\left(\frac{kT_{\rm e}}{m_{\rm e}c^2}\right) + 4\left(\frac{kT_{\rm e}}{m_{\rm e}c^2}\right)^2\right]\left[1 + \left(\frac{kT_{\rm e}}{m_{\rm e}c^2}\right)\right]^{-1}, \quad (11)$$

The above expressions are valid so long as the photon is soft, i.e., the radiation temperature is much less than the gas temperature. When the two temperatures are equal, thermodynamics guarantees that there is no energy transfer between gas and radiation. Similarly, when the radiation temperature is larger than the gas temperature, we expect energy to flow from the radiation to the gas. To allow for these effects, we modify the expression for $\widehat{G}^0$ in equation (8) to the following:

$$\begin{aligned}\widehat{G}^0 &= \rho a \kappa_{\rm a}(T_{\rm r}^4 - T_{\rm g}^4) - \kappa_{\rm es}\rho\widehat{E}\left[\frac{4k(T_{\rm g} - T_{\rm r})}{m_{\rm g}c^2}\right] \\ &\times \left[1 + 3.683\left(\frac{kT_{\rm g}}{m_{\rm g}c^2}\right) + 4\left(\frac{kT_{\rm g}}{m_{\rm g}c^2}\right)^2\right]\left[1 + \left(\frac{kT_{\rm g}}{m_{\rm g}c^2}\right)\right]^{-1}, \quad (12)\end{aligned}$$

where we have replaced T_e by $T_{\rm g}$. The negative sign in the Compton term is because gas cools when $T_{\rm g} > T_{\rm r}$. The cooling is proportional to the radiation energy density, $\widehat{E}$, and to the number of scatterings per unit time, $c\kappa_{\rm es}\rho$. The final two factors in square parentheses correspond to the approximate correction for relativistic temperatures given in equation (11). Apart from these factors, equation (12) is identical to the prescription used by Kawashima et al. (2009).

As far as the momentum equation is concerned, we assume that the Compton-scattered radiation is symmetric in the fluid frame and carries no net momentum (a fairly good approximation in the soft photon limit). Under this approximation, we keep equation (5) unchanged.

Thus, in this (simplest) version of thermal Comptonization, which we call "blackbody Comptonization," we solve equations (2) and (3) using equations (12) and (5), where $T_{\rm g}$ and $T_{\rm r}$ are given by equations (6) and (7), respectively. The main weakness of this approach is that it does not conserve photon number during scattering. Instead it assumes that the radiation is a perfect blackbody and uses equation (7) to obtain the radiation temperature.

2.3 Photon-conserving Comptonization

In the next approximation, which we call "photon-conserving Comptonization," we give up the assumption that the spectral shape is a perfect blackbody, but instead assume that the photons have a Bose-Einstein (BE) distribution in the fluid frame, described by two parameters: radiation temperature T_r and radiation chemical potential μ. Correspondingly, we keep track of not only the radiation energy and momentum density, $\widehat{E}$, $\widehat{F^i}$, but also the photon number density, $\widehat{n}$. This generalization allows us to include the effect of radiation dilution and spectral hardening.

Let us define the dimensionless photon energy, $x = h\nu/kT_{\rm r}$, and the dimensionless chemical potential, $\xi = \mu/kT_{\rm r}$. The angle-integrated BE distribution $f(x)dx$ of photons at temperature $T_{\rm r}$ is given by

$$f(x)dx = C(kT_{\rm r})^3 e^{-\xi}\frac{x^2 dx}{e^x - e^{-\xi}}, \qquad C \equiv \frac{8\pi}{c^3h^3}. \quad (13)$$

The radiation energy density and photon number density are then

$$\widehat{E} = C(kT_{\rm r})^4 e^{-\xi} I_E(\xi), \qquad I_E(\xi) = \int_0^\infty \frac{x^3 dx}{e^x - e^{-\xi}}, \quad (14)$$

$$\widehat{n} = C(kT_{\rm r})^3 e^{-\xi} I_N(\xi), \qquad I_N(\xi) = \int_0^\infty \frac{x^2 dx}{e^x - e^{-\xi}}. \quad (15)$$

In the Planck limit, i.e., when $\xi = 0$, we have $I_E = 6.493940$, $I_N = 2.404114$, while in the Wien limit, i.e., when $\xi \gg 1$, we have $I_E = 6$, $I_N = 2$.

Noting that $kT_{\rm r} \sim \widehat{E}/\widehat{n}$ and $e^{-\xi} \sim \widehat{n}^4/C\widehat{E}^3$, a little trial and error gives the following fitting function for the radiation temperature $T_{\rm r}$ in terms of $\widehat{E}$ and $\widehat{n}$,

$$kT_{\rm r} = \frac{\widehat{E}/\widehat{n}}{[3 - 2.449724(\widehat{n}^4/C\widehat{E}^3)]}. \quad (16)$$

The constants in the denominator have been chosen to give the correct result in the Planck and Wien limits. There is a small deviation at intermediate values of the chemical potential, but the fractional error in the temperature is at worst no more than 0.04%. In the present photon-conserving Comptonization approach, instead of using equation (7) which corresponds to blackbody Comptonization, we use equation (16) to calculate $T_{\rm r}$.

Note that the ratio $\widehat{E}/\widehat{n}$ is equal to $2.7012\,kT_{\rm r}$ in the blackbody limit and equal to $3\,kT_{\rm r}$ in the extreme Wien limit. This is a small enough difference that, in light of our other approximations, we could simply use the blackbody value of the ratio for all regimes. The key point is that the radiation temperature $kT_{\rm r}$ should be estimated via the ratio $\widehat{E}/\widehat{n}$ (with some reasonable coefficient) if we wish to satisfy photon conservation, whereas any approach based purely on equation (7) will violate photon conservation. In this work, we use the fitting function (16) when we model photon-conserving Comptonizaiton.[1]

Since we have introduced a new variable $\widehat{n}$, we need an evolution equation for this quantity. Here we use the fact that absorption removes photons, emission adds photons, and scattering leaves the number of photons unchanged. Thus, in the fluid frame, we write the rate of change of photon number density as

$$\dot{\widehat{n}} = -\rho\left[\left(\frac{\kappa_{\rm a}\widehat{E}/kT_{\rm r}}{3 - 2.449724(\widehat{n}^4/C\widehat{E}^3)}\right) - \left(\frac{4\pi\kappa_{\rm a}\widehat{B}/kT_{\rm g}}{2.701178}\right)\right]. \quad (17)$$

The evolution equation for the photon number density n is then written as

$$(nu^\mu_r)_{;\mu} = \dot{\widehat{n}}, \quad (18)$$

where $u^\mu_{\rm r}$ is the four-velocity of the radiation frame, and we have used the fact that $\dot{\widehat{n}}$ is a frame-invariant quantity (because $\dot{n} = dN/dt\,dx_1dx_2dx_3$, and both the numerator and the denominator are relativistic invariants).

In summary, under the photon-conserving Comptonization approximation, we solve equations (2), (3) and (18), using equations (5), (12) and (17), where $\widehat{B}$ is given by equation (6) and $T_{\rm r}$ is given by equation (16).

3 NUMERICAL METHODS

To solve equations 2-5, we use the general relativistic radiation magnetohydrodynamical (GRRMHD) code KORAL (Sądowski et

[1] Because of the negative sign in the denominator of equation (16), the function can sometimes diverge and behave unphysically. This potential pathology (which has not been an issue in any of the simulations we have run so far, including those presented here) can be fixed by resetting the denominator to its minimum value of 2.7012 whenever it tries to go lower, or by choosing a different form of the fitting function (Jonathan McKinney, private communication).

al. 2013, 2014), which employs a Godunov scheme to evolve the conservation equations in a fixed, arbitrary spacetime using finite-difference methods. The magnetic field is evolved via the induction equation, with the divergence-free criterion being enforced using a flux-constrained (Tóth 2000) scheme as described in Gammie et al. (2003). The radiation field is evolved through its energy density and flux, and the radiation stress-energy tensor is closed by means of the M1 closure scheme (Levermore 1984). For details of the basic method see Sądowski et al. (2014).

For the purpose of this work we adopt a simple prescription for the absorption opacity κ_a (Kato et al. 2008),

$$\kappa_{\rm a} = 6.4 \times 10^{22}\, \rho T_{\rm g}^{-7/2}\, {\rm cm}^2 {\rm g}^{-1}. \quad (19)$$

Note that the absorption opacity should in principle be a function of both gas and radiation temperatures. We ignore this complication here. Similarly, in the spirit of keeping things simple, we ignore the fact that the rate of change of photon number by absorption and emission is generally more complicated than the prescription given in equation (17). These issues will be dealt with more accurately in future studies. For the scattering opacity we use

$$\kappa_{\rm es} = 0.34\, {\rm cm}^2 {\rm g}^{-1}. \quad (20)$$

Thermal Comptonization within the "blackbody" approximation (Section 2.2) has already been included in KORAL and has been described in a previous paper (Sądowski et al. 2015a). Implementing that scheme does not require any modification to the basic algorithm in KORAL; we merely need to modify the time component of the fluid frame four-force, which describes the rate of exchange of energy between gas and radiation, according to equation (12). The corresponding radiation four-force density G^μ then takes the form (Sądowski et al. 2014),

$$G^\mu_{\rm Compt} = \widehat{G}^0_{\rm Compt} u^\mu, \quad (21)$$

where,

$$\widehat{G}^0_{\rm Compt} = -\kappa_{\rm es}\rho\widehat{E}\left[\frac{4k(T_{\rm g}-T_{\rm r})}{m_{\rm g}c^2}\right] \times\left[1+3.683\left(\frac{kT_{\rm g}}{m_{\rm g}c^2}\right)+4\left(\frac{kT_{\rm g}}{m_{\rm g}c^2}\right)^2\right]\left[1+\left(\frac{kT_{\rm g}}{m_{\rm g}c^2}\right)\right]^{-1} \quad (22)$$

The photon-conserving Comptonization scheme introduced in this work (Section 2.3), on the other hand, requires a modified algorithm. One more conserved quantity – the photon number density n – has to be evolved, for which we use equation (18). The source term on the right hand side of (18) describes the change of photon number due to emission and absorption by the gas, and is proportional to the absorption opacity $\kappa_{\rm a}$. As in the case of other radiative source terms (equations. 4-5), this term may become stiff in an optically thick medium. Therefore, it is necessary to apply it in an implicit way. For this purpose we modify the original semi-implicit operator (Sądowski et al. 2013), which applies the standard radiative source terms, to include the evolution of the photon number density. The set of equations solved in the implicit step is now,

$$(\rho u^t)_{(i+1)} - (\rho u^t)_{(i)} = 0, \quad (23)$$

$$T^t_{\nu,(i+1)} - T^t_{\nu,(i)} = \Delta t G_{\nu,i+1}, \quad (24)$$

$$R^t_{\nu,(i+1)} - R^t_{\nu,(i)} = -\Delta t G_{\nu,i+1}, \quad (25)$$

$$(nu^t_{\rm r})_{(i+1)} - (nu^t_{\rm r})_{(i)} = \dot{\widehat{n}}_{(i+1)}, \quad (26)$$

where subscripts (i) and $(i+1)$ indicate values at the beginning and end of the current time step, respectively. Due to the symmetry of the problem, it is enough to iterate just one set of primitives, either radiative or hydrodynamical, extended by the photon number density, and to use the conservation of energy and momentum to recover the remaining quantities.

The new system of equations is solved for values at the new moment of time (denoted by $(i+1)$) using the Newton-Raphson method in five dimensions. The computational cost increases because of the extra dimension by a factor of $\lesssim 2$ in most cases.

Table 1. Model parameters

$M_{\rm BH}$	$10M_\odot$
a_*	0.0
$\rho_{\rm max}$	4.3×10^{-3} g/cm^3
$\beta_{\rm max}$	10.0
N_R x N_θ	252 x 234
$R_{\rm min}$ / $R_{\rm max}$ / R_0 / H_0	1.85 / 1000 / 0 / 0.6
$t_{\rm max}$	48,000
$\langle\dot{M}\rangle/\dot{M}_{\rm Edd}$	10.2 (blackbody Compt.)
	11.2 (N-Compt.)
	9.2 (no Compt.)

$\rho_{\rm max}$ - maximal density of the initial torus
$\beta_{\rm max}$ - maximal value of initial total to magnetic pressure ratio
$t_{\rm max}$ - duration of simulation

4 SIMULATIONS

4.1 Initial setup

To assess how important the proper treatment of Comptonization is for accretion disks we carried out a set of simulations of supercritical accretion flows on a $10M_\odot$ BH. In order to obtain a relatively large radial range of inflow/outflow equilibrium, we decided to perfom the simulations in 2D assuming axisymmetry. The poloidal magnetic field was maintained by means of the mean-field magnetic dynamo model of Sądowski et al. (2015a).

We performed three simulations, each initiated in exactly the same way as described in Sądowski et al. (2014), with parameters given in Table 1. The only difference between the runs was the way Comptonization was treated: (i) basic "blackbody Comptonization" prescription (Section 2.2), (ii) improved "photon-conserving Comptonization" (Section 2.3), (iii) no Comptonization at all. For the run with photon-conserving Comptonization we had to specify the initial photon density. Because the radiation and gas in the initial torus satisfy local thermal equilibrium, we set the radiation and gas temperatures to be equal and set the photon number density according to the blackbody formula,

$$\widehat{n} = \frac{a_{\rm rad}T^3}{2.7012k_{\rm B}}. \quad (27)$$

Hereafter, we use the gravitational radius $R_{\rm g} = GM/c^2$ as the unit of length, and R_g/c as the unit of time.

4.2 Accretion flow properties

All three simulations were run up to a final time of $t_{\rm max} = 48,000$. The region of inflow/outflow equilibrium extended up to a radius $R \approx 30$ in the equatorial plane, and to a much larger distance in the funnel region near the axis (where the radial velocity of the outflowing gas is much higher, $\gtrsim 0.1c$). The mean accretion rate for all the models was $\sim 10\dot{M}_{\rm Edd}$ (Table 1). The time history of the mass accretion rate through the BH horizon is shown in Fig. 1. Although

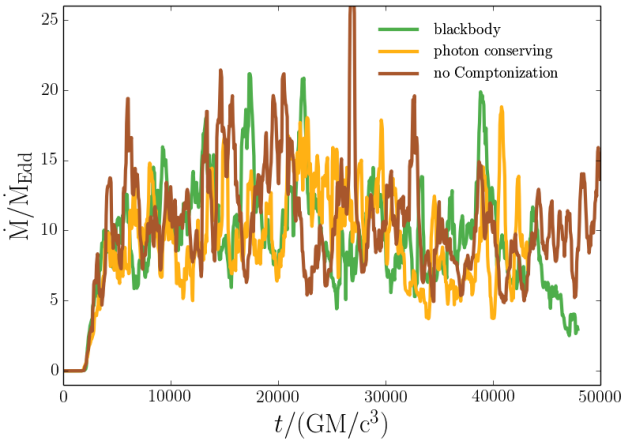

Figure 1. Mass accretion rate at the BH as a function of time for the three models considered.

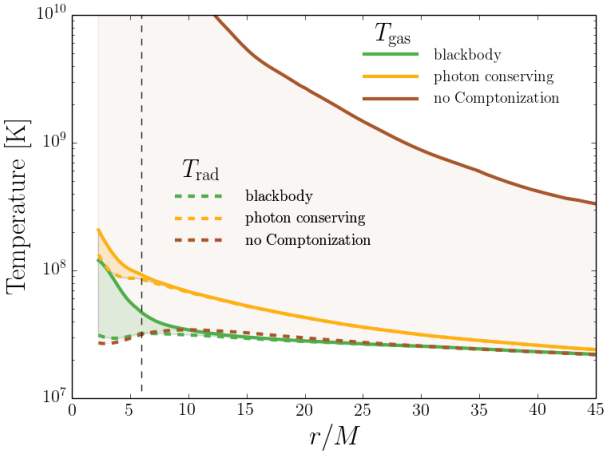

Figure 3. Radial profiles of density weighted gas (solid) and radiation (dashed lines) temperatures in the three models. The shaded regions reflect the difference between the two temperatures.

the profiles are highly variable, as expected for a turbulent accretion flow, there are no significant differences in the three profiles. This suggests that the precise treatment of Comptonization has little impact on the the gross dynamical properties of the gas.

A similar conclusion is reached when comparing the time- and ϕ-averaged distributions of density in the poloidal plane, shown in the top row of panels in Fig. 2. From the left, the three panels correspond to blackbody Comptonization, photon-conserving Comptonization, and no Comptonization, respectively. In all three simulations, the accretion flow is geometrically thick, with an average density scale height $H/R \sim 0.3$. The densities at the equatorial plane are similar in all three runs, with $\rho \sim 10^{-3}$ g s^{-1}. The dashed lines in the panels show the location of the scattering photospheres as measured from infinity along fixed polar angle θ. In all models the polar region is optically thin (i.e., the observer looking into the funnel can directly see radiation coming from the vicinity of the BH horizon). The size of this region is largest for the photon-conserving model, but the difference is not large.

Although the densities in the three runs are similar, the gas and radiation temperatures, shown respectively in the second and third rows of panels in Fig. 2, are significantly different. In scattering dominated media, and in stellar mass BH accretion disks in particular, Comptonization often dominates the energy transfer rate between the gas and radiation; without Comptonization, the coupling is very weak.

Turbulent dissipation in the disk heats the gas, the rate of heating depending mostly on the properties and evolution of the MHD turbulence, which is insensitive to the way we treat Comptonization. When the gas subsequently cools, the dissipated heat energy is transfered to radiation. To sustain a given rate of energy transfer from gas to radiation, one can either have efficient coupling, with gas and radiation temperatures close to each other, or weak coupling, with a large difference in the two temperatures. In the case of the simulation with no Comptonization (right panels), the coupling is weak, therefore the gas temperature becomes very large. This effect is significant in the inner regions of the disk and is particularly evident in the coronal and polar regions, where the gas temperature exceeds 10^{10} K, while the radiation temperature stays around 10^7 K. In contrast, for the two models that allow Compton coupling, viz., blackbody Comptonization and photon-conserving Comptonization, the gas temperature is much lower, and is also closer to the radiation temperature, reflecting the fact that the coupling between the gas and the radiation field is strong. As in the case of the no Comptonization model, the gas temperature tends to be higher than the radiation temperature here as well, but the difference, even in the coronal region, is no longer very extreme.

Radial profiles of the gas and radiation temperatures (these are density-weighted, and therefore are dominated by the gas in the disk interior rather than the corona) are shown in Fig. 3. The average gas temperature at radius $R = 15$ is approximately 5×10^9, 6×10^7, and 3×10^7 K for models with no, photon-conserving, and blackbody Comptonization, respectively. The overheating of the gas in the no Comptonization model is dramatically evident. The other two models (which include Comptonization) have lower gas and radiation temperatures and the two temperatures are nearly equal in the bulk of the disk ($R \gtrsim 10$). The actual temperatures are, however, not the same for the two models. The photon-conserving model is hotter by a factor of 2 (measured by either gas or radiation temperature). This is a significant difference and will have a noticeable effect on the spectral properties of the escaping radiation.

The blackbody Comptonization and no Comptonization models assume that the radiation spectrum is blackbody. Therefore, in these models the radiation temperature $T_{\rm r}$ is a function only of the radiative energy density in the fluid frame,

$$T_{\rm r} = \left(\frac{\widehat{E}}{a}\right)^{1/4} \equiv T_{\rm r,BB}. \tag{28}$$

For the photon-conserving Comptonization model, however, we track the number density of photons and use equation (16) to compute $T_{\rm r}$. This temperature is equal to $T_{\rm r,BB}$ only in those regions of the flow where the radiation happens to be black body, e.g., deep inside the disk. In other regions, the local number density of photons deviates from the blackbody value, and so do the temperature and spectrum. We define the color correction factor as the ratio of the real radiation temperature to the blackbody temperature,

$$f_{\rm col} = \frac{T_{\rm r}}{T_{\rm r,BB}}. \tag{29}$$

Values of $f_{\rm col}$ larger than unity correspond to a radiation spectrum that is harder than blackbody. Under the gray approximation we have adopted in this work, we do not have detailed information on

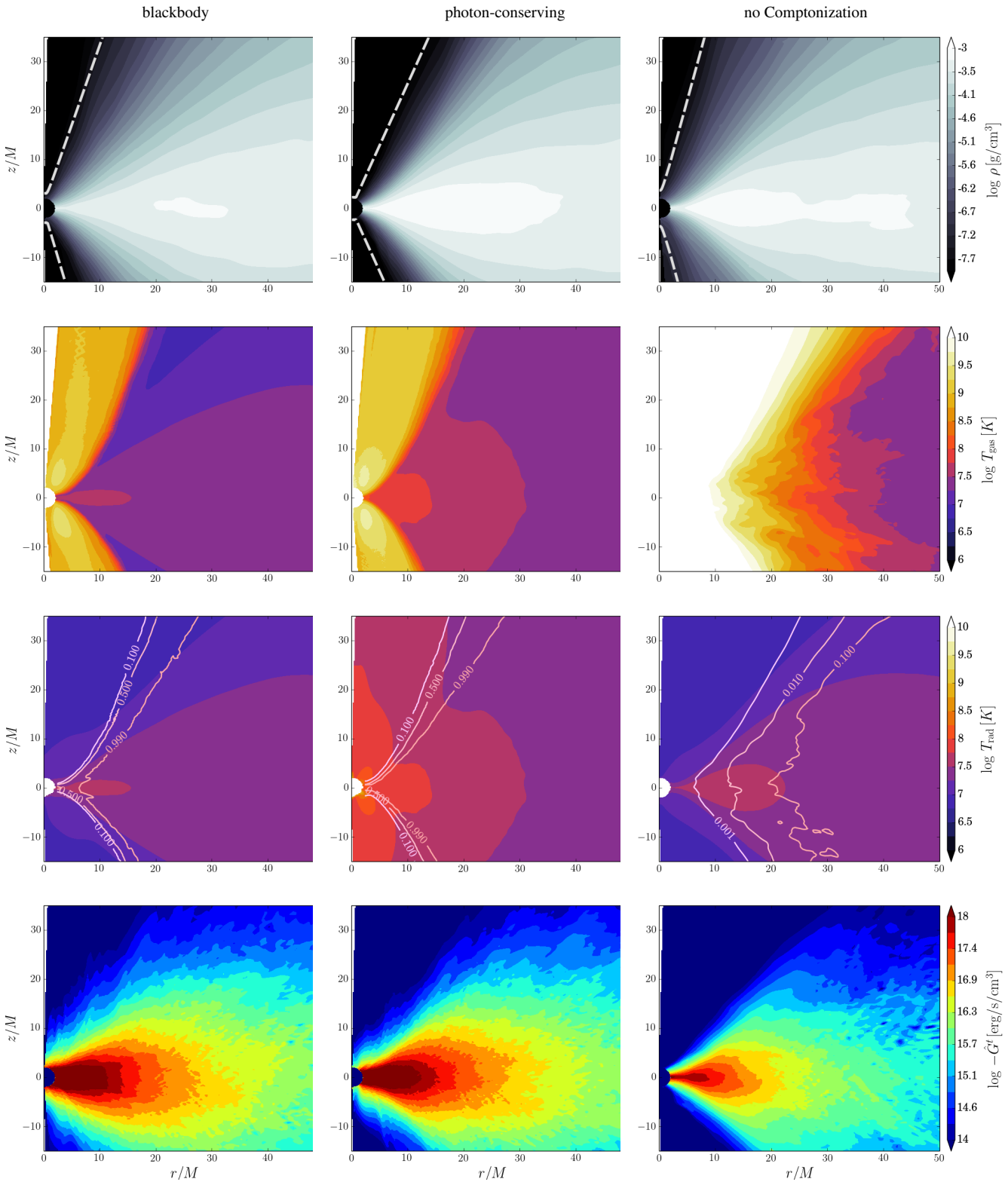

Figure 2. Distributions of density (top row), gas temperature (second row) radiation temperature (third row), and cooling rate (bottommost row) for models with blackbody Comptonization (left), photon-conserving Comptonization (middle), and no Comptonization (right panels). Plots correspond to data averaged over $t = 24000 \div 48000$. The dashed lines in the density plots reflect the location of the scattering photosphere as measured from infinity along fixed polar angle. The contours on the radiation temperature plots (third row) reflect the radiation to gas temperature ratio.

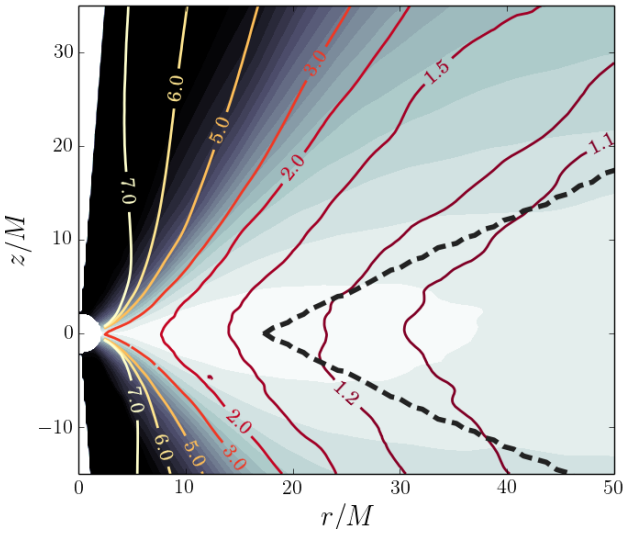

Figure 4. Color correction factor $f_{\rm col}$ (equation 29) corresponding to the photon-conserving Comptonization model. The colors reflect the distribution of gas density and the black dashed line shows the location of the effective photosphere (equation 30).

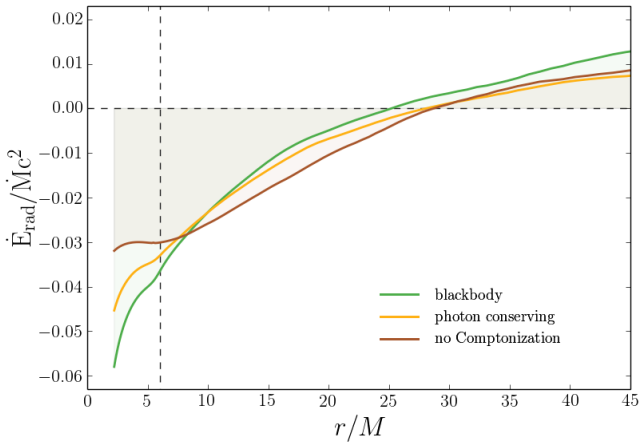

Figure 5. Radiative luminosity $\dot{E}_{\rm rad}$ (equation 31) as a function of radius for the three models.

the spectral shape of the radiation field. Therefore, spectral distortion from blackbody is described by a single number $f_{\rm col}$. More detailed, frequency-dependent radiative transfer is required if we wish to obtain additional information.

By definition, the color correction factor (equation 29) is equal to unity for the blackbody and no-Comptonization models, since the radiation spectrum is assumed to be blackbody. In the photon-conserving Comptonization model, however, it can (and does) deviate from unity. The contours in Fig. 4 show the color correction factor for this model plotted on top of the gas density distribution. The black dashed line shows the location of the effective photosphere, estimated by integrating the effective optical depth from the axis along θ at fixed *radius* and identifying the angle at which it equals 2/3:

$$\int_0^\theta \rho \sqrt{\kappa_{\rm a}(\kappa_{\rm a}+\kappa_{\rm es})}\,\sqrt{g_{\theta\theta}}\,d\theta' = 2/3. \qquad (30)$$

Deep in the disk and at large radii ($R \gtrsim 30$), where the disk is opticaly thick to both scattering and absorption, $f_{\rm col}$ is close to unity and the radiation spectrum is close to blackbody. The color correction increases (the spectrum becomes harder) as the radiation gets closer to the disk surface — the photons are up-scattered by hot gas and gain energy. Near the edge of the funnel, the color correction factor reaches $f_{\rm col} \approx 5.0$, which reflects how strongly scattering modifies the radiation field.[2] This large value suggests that the spectrum would be strongly dominated by a Compton hump, and the original black body component would be insignificant (compare Kawashima et al. 2012).

The rate of energy transfer from gas to radiation is the cooling rate of the gas and describes how effectively the heat energy released by turbulent dissipation goes into the radiation field. The bottommost panels of Fig. 2 show the distribution of the time-averaged cooling rate for the three models. For all three simulations, the highest rates of energy transfer are at the equatorial plane and in the innermost region ($R \lesssim 15$). However, the vertical extent of this region as well as the magnitude of the cooling differ. The no Comptonization model shows the least amount of cooling both in the funnel region near the axis and at the equatorial plane. For the thermal and photon-conserving Comptonization models, the cooling region extends further towards the axis and the magnitude of the cooling rate is also larger.

Because accretion flows are quasi-stationary, the energy transfered from gas to radiation via cooling must be removed in some fashion. In optically thick disks, this can happen in two ways — either by radiation flowing out of the disk or by radiation being trapped in the gas and carried into the BH with the flow (advected). Fig. 5 is a plot of the radiative luminosity as a function of radius for the three models, calculated as follows,

$$\dot{E}_{\rm rad} = \int_2^R R^r_t\,\sqrt{-g}\,{\rm d}A, \qquad (31)$$

where $\sqrt{-g}$ is the metric determinant and ${\rm d}A = 2\pi r^2 d\theta$ is a differential surface element at radius r. Negative values of this quantity correspond to regions where radiation advection into the BH dominates. The radius where $\dot{E}_{\rm rad} = 0$ reflects the location of the effective trapping radius of the accretion flow.

All three runs show significant advection of photons. Only outside radius $R \approx 25$ does the net flux of radiation point outward. To estimate the total amount of energy put into the radiation field we take the luminosity in inflowing photons at the BH and add it to the luminosity in outflowing photons at radius $R = 45$. The total energy release in radiation is roughly 7%, 6%, and 4%$\dot{M}c^2$ for the blackbody, photon-conserving, and no Comptonization models, respectively[3]. These numbers are in agreement with the discussion of the cooling rate in the previous paragraphs, viz., not including Comptonization underestimates the cooling rate.

By taking the radial derivative of the radiation luminosity $\dot{E}_{\rm rad}$, we obtain the local photon generation rate or the gas cooling rate. This quantity is shown in Fig. 6. The emission profiles more or less overlap in the outer ($R > 15$) region but are significantly different

[2] It is interesting to note that similar values of the color correction factor were obtained by Kawaguchi (2003) who estimated Comptonized spectra of slim accretion disks.

[3] We stress here that these numbers do not correspond to the standard definition of radiative efficiency, which includes only radiation escaping to a distant observer.

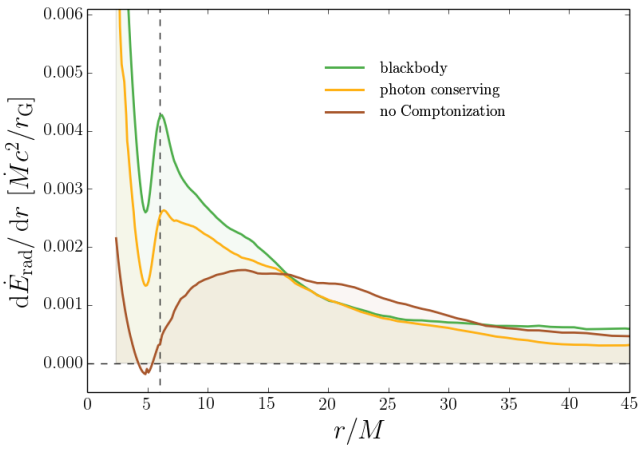

Figure 6. Profiles of radiative emission per unit radius for the three models.

inside that radius. The maximum amount of energy is put into radiation in the blackbody Comptonization model, and the least when Comptonization is not taken into account. In the latter model, there is hardly any emission inside the marginally stable orbit.

5 DISCUSSION

In this work we have introduced an improved method for treating Comptonization in computational fluid dynamics. The suggested approach conserves the number of photons and allows for a non-blackbody spectrum of radiation. It is fully covariant and may be applied to simulations performed in general relativity. However, the method is still very approximate, since it assumes a specific spectral shape for the radiation, viz., a Bose-Einstein distribution function (eq. 13). Also, the proposed algorithm is valid only for gray radiative transfer. Nevertheless, we believe this "photon-conserving Comptonization" method is a significant improvement over the traditional "blackbody Comptonization method".

To assess the effect of various treatments of Comptonization in modeling accretion disks, we performed a set of three simulations corresponding to a super-critical disk accreting at $10\dot{M}_{\mathrm{Edd}}$. We implemented the new photon-conserving approach (described in detail in Section 2.3) as well as blackbody Comptonization (Section 2.2) and considered also a model with no Comptonization. We find that the density distribution and the accretion rate are insensitive to the way we model Comptonization, whereas the gas temperature and the properties of the radiation field depend strongly on which version of Comptonization we use. In particular, simulations with no Comptonization produce unphysically high gas temperatures. This is because of inefficient coupling between gas and radiation. The blackbody approach, on the other hand, noticeably underestimates the gas and radiation temperatures. In making these statements, we are working on the assumption that the photon-conserving model, being the most sophisticated of the three, is closest to the true solution.

By comparing the three simulations we find that the impact of Comptonization is not limited to the coronal regions (as claimed by some authors), but that it actually affects the gas properties throughout the disk, even deep inside the effective photosphere. With no Comptonization at all, the coupling between gas and radiation comes only from the absorption opacity, which requires significantly different gas and radiation temperatures. With Comptonization, the optically thick gas in the bulk of the disk is at lower temperatures, closer to the radiation temperature.

The photon-conserving model provides one additional piece of information compared to the other two models, viz., the color correction factor f_{col} as a function of position. This factor, which measures the ratio of the radiation temperature to an effective blackbody temperature (eq. 29), describes the amount of spectral hardening caused by scattering and Comptonization. We find that f_{col} can deviate substantially from unity, and can be as large as 5 or 6 at the photosphere inside the funnel. Such high color correction factors will characterize radiation escaping through the polar funnel region, and will be visible to observers viewing at small polar angles. For larger inclinations, most of the observed radiation would come from the disk photosphere located far from the BH (this region is not resolved in our simulations) and would likely not show such strong Comptonization.

Another quantity that is significantly affected by the version of Comptonization that one uses is the amount of cooling, which determines the ultimate luminosity (both in advected and escaping photons). The blackbody and no-Comptonization models over- and under-estimate the cooling rate, respectively.

Taking into account the modest computational cost of the photon-conserving Comptonization approach, we recommend using it in simulations of accretion disks. It is true that blackbody Comptonization reproduces reasonably well the dynamical properties of the accretion flow and the cooling rate. However, the gas and radiation temperatures obtained via this approach are significantly under-estimated. Therefore, this model cannot be trusted for applications in which the temperature is of interest, e.g., spectral modeling.

To complete this study we need to assess how the treatment of Comptonization affects the spectrum as seen by a distant observer. This requires post-processing with a multi-dimensional radiative transfer solver that works in general relativity and allows for frequency-dependent opacity (e.g., Zhu et al. 2015) and Comptonization.

6 ACKNOWLEDGEMENTS

The authors thank Jonathan McKinney for helpful discussions and comments. AS acknowledges support for this work by NASA through Einstein Postdoctotral Fellowship number PF4-150126 awarded by the Chandra X-ray Center, which is operated by the Smithsonian Astrophysical Observatory for NASA under contract NAS8-03060. AS thanks Harvard-Smithsonian Center for Astrophysics for its hospitality. RN was supported in part by NSF grant AST1312651 and NASA grant TCAN NNX14AB47G. The authors acknowledge computational support from NSF via XSEDE resources (grant TG-AST080026N), and from NASA via the High-End Computing (HEC) Program through the NASA Advanced Supercomputing (NAS) Division at Ames Research Center.

REFERENCES

Abramowicz, M. A., Czerny, B., Lasota, J. P., & Szuszkiewicz, E. 1988, Astrophysical Journal, 332, 646
Balbus, S. A., & Hawley, J. F. 1998, Reviews of Modern Physics, 70, 1
Davis, S. W., Blaes, O. M., Hubeny, I., & Turner, N. J. 2005, Astrophysical Journal, 621, 372
Fabian, A. C. 2012, Ann. Rev. Astron. Asrophys., 50, 455

Fragile, P. C., Olejar, A., & Anninos, P. 2014, arXiv:1408.4460
Gammie, C. F., McKinney, J. C., & Tóth, G. 2003, Astrophysical Journal, 589, 444
Hubeny, I., & Lanz, T. 1995, Astrophysical Journal, 439, 875
Hubeny, I., & Hubeny, V. 1997, Astrophysical Journal Letters, 484, L37
Hubeny, I., Blaes, O., Krolik, J. H., & Agol, E. 2001, Astrophysical Journal, 559, 680
Jiang, Y.-F., Stone, J. M., & Davis, S. W. 2014, Astrophysical Journal Suppl. Ser., 213, 7
Jiang, Y.-F., Stone, J. M., & Davis, S. W. 2014, Astrophysical Journal, 796, 106
Kato, S., Fukue, J., & Mineshige, S. 2008, Black-Hole Accretion Disks — Towards a New Paradigm —, 549 pages, including 12 Chapters, 9 Appendices, ISBN 978-4-87698-740-5, Kyoto University Press (Kyoto, Japan), 2008.,
Kawaguchi, T. 2003, Astrophysical Journal, 593, 69
Kawashima, T., Ohsuga, K., Mineshige, S., et al. 2009, Publications of the Astronomical Society of Japan, 61, 769
Kawashima, T., Ohsuga, K., Mineshige, S., et al. 2012, Astrophysical Journal, 752, 18
King, A., & Pounds, K. 2015, arXiv:1503.05206
Levermore, C. D. 1984, Journal of Quantitative Spectroscopy and Radiative Transfer, 31, 149 2
McClintock, J. E., Narayan, R., Davis, S. W., et al. 2011, Classical and Quantum Gravity, 28, 114009
McKinney, J. C., Narayan, R., Sądowski, A., & Tchekhovskoy, A. 2013, Monthly Notices of the Royal Astronomical Society, submitted
M oller, A., A. Sądowski 2015, in prep
Novikov, I. D., & Thorne, K. S. 1973, Black Holes (Les Astres Occlus), 343
Ohsuga, K., Mineshige, S., Mori, M., & Yoshiaki, K. 2009, Publications of the Astronomical Society of Japan, 61, L7
Ohsuga, K., & Mineshige, S. 2011, Astrophysical Journal, 736, 2
Pozdnyakov, L. A., Sobol, I. M., & Syunyaev, R. A. 1983, Astrophysics and Space Physics Reviews, 2, 189
Rybicki, G. B., & Lightman, A. P. 1979, New York, Wiley-Interscience, 1979. 393 p.,
Sądowski, A. 2011, Ph.D. Thesis, Nicolaus Copernicus Astronomical Center, Polish Academy of Sciences, arXiv:1108.0396
Sądowski, A., Narayan, R., Tchekhovskoy, A., & Zhu, Y. 2013a, Monthly Notices of the Royal Astronomical Society, 429, 3533
Sądowski, A., Narayan, R., McKinney, J. C., & Tchekhovskoy, A. 2014, Monthly Notices of the Royal Astronomical Society, 439, 503
Sądowski, A., Narayan, R., Tchekhovskoy, A., Abarca, D., Zhu, Y., & McKinney J. C. . 2015a, Monthly Notices of the Royal Astronomical Society, 447, 49
Sadowski, A., & Narayan, R. 2015b, arXiv:1503.00654, MNRAS, submitted
Sadowski, A., & Narayan, R. 2015c, MNRAS, submitted
Shakura, N. I., & Sunyaev, R. A. 1973, A&A, 24, 337
Straub, O., Bursa, M., Sądowski, A., et al. 2011, Astronomy & Astrophysics, 533, A67
Tóth, G. 2000, Journal of Computational Physics, 161, 605
Zhu, Y., Narayan, R., Sadowski, A., & Psaltis, D. 2015, Monthly Notices of the Royal Astronomical Society, 451, 1661